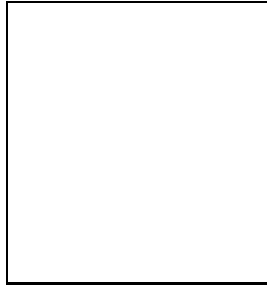


# DIBOSON PRODUCTION CROSS-SECTIONS AT $\sqrt{s} = 1.96$ TeV

AIDAN ROBSON

on behalf of the CDF and D0 Collaborations

*Department of Physics, Keble Road,  
Oxford OX1 3RH, UK*



Recent results of  $W\gamma$ ,  $Z\gamma$  and  $WW$  cross-section measurements in the electron and muon channels are reported from  $p\bar{p}$  collisions at  $\sqrt{s} = 1.96$  TeV recorded by the CDF and D0 collaborations. Total cross-sections and kinematic distributions are found to be consistent with Standard Model expectations.

## 1 Introduction

Diboson cross-section measurements provide tests of the Standard Model and in particular a way of studying boson self-couplings. The three groups of analysis presented here,  $W\gamma$ ,  $Z\gamma$  and  $WW$ , are complementary in the sense of being rather different from each other statistically, in their backgrounds, and in their leading systematic uncertainties. From the point of view of studying boson self-couplings the analyses also complement one another. Whereas examining  $WW$  production probes the  $WWZ$  and  $WW\gamma$  vertices, which are difficult to separate experimentally, measuring  $W\gamma$  production probes only the  $WW\gamma$  vertex.

In addition to the intrinsic interest of the measurements, a solid understanding of diboson production is also important for other physics: in  $t\bar{t}$  measurements if the  $W$ s from the  $t$ -quark both decay leptonically the signature is very similar to a  $WW$  event as identified in these analyses; and a heavy Higgs would favour decay to two heavy bosons.

Inclusive  $W$  and  $Z$  cross-section measurements from CDF and D0 are reported elsewhere in these proceedings<sup>1</sup>. The recent preliminary  $W$  and  $Z$  cross-sections from CDF are precise to 2% (neglecting the common luminosity error), which alongside their excellent agreement with NNLO predictions provides the basis of our understanding for measuring the diboson cross-sections. The results presented here are very recent, and in particular the  $W\gamma$  results from D0 and the  $WW$  results from CDF are new for this conference.

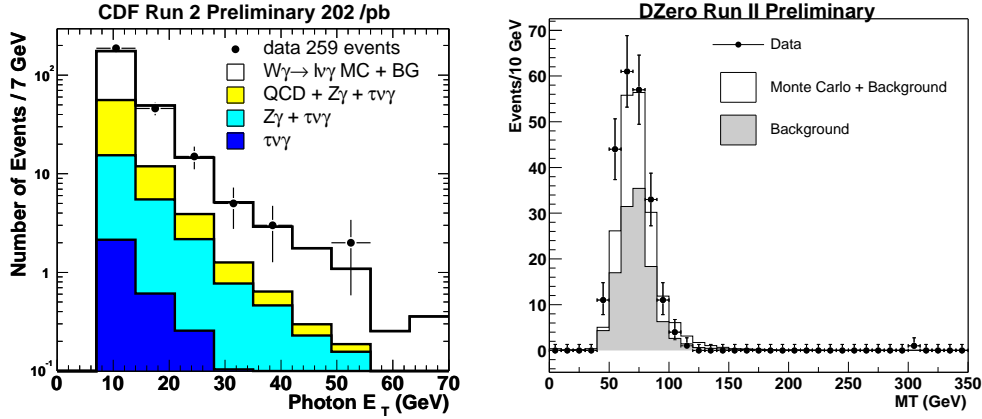


Figure 1: (left)  $E_T^\gamma$  for CDF's  $W\gamma$  candidate events; (right)  $m_{T(\ell,\nu)}$  for D0's  $W\gamma$  candidate events.

## 2 $p\bar{p} \rightarrow W\gamma \rightarrow \ell\nu\gamma$ cross-section

CDF and D0 report preliminary measurements of the  $W\gamma$  production cross-section using electron and muon decay channels. In each case the initial selection of the  $W$  follows closely that of the inclusive cross-section measurement. CDF selects electron candidates from the central region of the detector ( $|\eta| < 1.1$ ) that are isolated in the calorimeter and have  $E_T > 25$  GeV. Requirements are made on the amount of hadronic energy associated with the electromagnetic cluster, on the electromagnetic shower shape, and on the quality and matching of the associated track. Muon candidates are selected in  $|\eta| < 1.1$  and are required to be isolated and to have small amounts of energy deposited in the calorimeters. The muon candidate tracks are required to have  $p_T > 20$  GeV/ $c$ , to be well-matched to hits in the muon chambers, and to be inconsistent with cosmic rays. In addition to the lepton selection, candidate events are required to have  $E_T > 20$  GeV in the muon channel, and  $E_T > 25$  GeV in the electron channel. A requirement is made on the transverse mass  $m_{T(\ell,\nu)}$ , and to reject  $Z$ s a veto is made on second high- $p_T$  tracks in muon events.

The  $W\gamma$  cross-section must be defined in a particular kinematic region, and CDF chooses  $E_T^\gamma > 7$  GeV and a separation between lepton and photon  $\Delta R_{\ell\gamma} > 0.7$ , where  $(\Delta R)^2 = (\Delta\eta)^2 + (\Delta\phi)^2$ . The photon selection is similar to the electron selection but makes further use of the electromagnetic shower profile information, and in addition to requiring calorimeter isolation a limit is made on the number and energy of charged tracks pointing towards the cluster. The fake photon background is large and understanding the probability for a jet to fake a photon is one of the principal challenges of this measurement.

In  $202\text{pb}^{-1}$  CDF finds 259 events in the combined electron and muon channels, compared with a Standard Model expectation of  $255.6 \pm 2.1_{\text{stat}} \pm 26.4_{\text{sys}}$  events. The preliminary measured cross-section is  $\sigma \cdot Br(W\gamma \rightarrow \ell\nu\gamma) = (19.7 \pm 1.7_{\text{stat}} \pm 2.0_{\text{sys}} \pm 1.1_{\text{lum}})$  pb, to be compared with a NLO prediction<sup>2</sup> of  $(19.3 \pm 1.4)$  pb.

The  $E_T^\gamma$  distribution is shown in Fig. 1. A similar analysis, although with no  $m_{T(\ell,\nu)}$  requirement, using Run I CDF data found an excess at high  $E_T^\gamma$  and it is interesting to see that no such excess is observed in the current dataset.

The lepton selection used by D0 uses techniques similar to those described above for the CDF analysis, although with an extended coverage of  $|\eta| < 2.3$  for electrons and  $|\eta| < 2.0$  for muons. Candidate electrons are required to have a cluster isolated in the calorimeter with high electromagnetic fraction and a matching track. Muon candidates are required to be isolated in the calorimeter and to have a central track matching a track in the muon spectrometer.

The photon is required to be central,  $|\eta| < 1.1$ , and the total  $p_T$  of tracks pointing towards the photon candidate cluster is limited. The measurement is made in the kinematic region  $E_T^\gamma > 8 \text{ GeV}$  and  $\Delta R_{\ell\gamma} > 0.7$ . In total, 146 events are found in  $162 \text{ pb}^{-1}$  of data in the electron channel compared with a Standard Model expectation of  $142 \pm 17$  events, and 77 events are found in  $82 \text{ pb}^{-1}$  of data in the muon channel, compared with an expectation of  $67 \pm 13$  events. This leads to a preliminary cross-section measurement in the electron and muon channels of  $\sigma \cdot Br(W\gamma \rightarrow \ell\nu\gamma) = (19.3 \pm 2.7_{\text{stat}} \pm 6.1_{\text{sys}} \pm 1.2_{\text{lum}}) \text{ pb}$ , to be compared with a NLO prediction<sup>2</sup> of  $(16.4 \pm 0.4) \text{ pb}$ . The  $m_{T(\ell,\nu)}$  distribution of the candidate events is shown in Fig. 1.

### 3 $p\bar{p} \rightarrow Z\gamma \rightarrow \ell\ell\gamma$ cross-section

CDF reports a preliminary measurement of the  $Z\gamma$  production cross-section using around  $200 \text{ pb}^{-1}$  of data. The first leg of  $Z$  candidates is selected identically to the lepton in the  $W\gamma$  analysis described above. Somewhat looser requirements are made on the second leg, and the coverage of the analysis is extended by allowing a second electron leg to be in the forward regions of the detector,  $1.2 < |\eta| < 2.8$ , in which case a matching silicon track is required. An invariant mass cut  $m_{\ell\ell} > 40 \text{ GeV}/c^2$  is applied, and in the case of two central electrons or two muons, an opposite-charge requirement is made on the tracks. A photon is selected in the same way as for the  $W\gamma$  analysis, and as in the  $W\gamma$  measurement the photon background has a large uncertainty. However  $Z$  selection has much smaller background than  $W$  selection, and so the total background in the  $Z\gamma$  analysis is small. In  $202 \text{ pb}^{-1}$  of data, 69  $Z\gamma$  candidate events are found compared with a Standard Model expectation of  $70.5 \pm 4.0$  events. The preliminary measured cross-section is  $\sigma \cdot Br(Z\gamma \rightarrow \ell\ell\gamma) = (5.3 \pm 0.6_{\text{stat}} \pm 0.3_{\text{sys}} \pm 0.3_{\text{lum}}) \text{ pb}$ , to be compared with a NLO prediction<sup>2</sup> of  $(5.4 \pm 0.3) \text{ pb}$ . Kinematic distributions for the  $Z\gamma$  candidates, for example the photon  $E_T$  spectrum given in Fig. 2, show good agreement between data and Standard Model expectation.

### 4 $p\bar{p} \rightarrow WW \rightarrow \ell\nu\ell\nu$ cross-section

CDF reports two measurements of the  $WW$  cross-section: the first making tight lepton cuts aiming for high purity, and the second with a rather more open acceptance with the aim of increasing statistics.

The ‘tight lepton’ analysis selects two leptons according to criteria similar to those described in Section 2, except with a universal  $E_T$  cut of  $20 \text{ GeV}$ . Additional muon coverage is included by allowing second muon candidates that do not point towards muon chambers and thus could not have a matching stub. Leptons are required to have opposite charge, and candidate events to have  $\cancel{E}_T > 25 \text{ GeV}$ . To reduce fake  $\cancel{E}_T$  from mismeasured leptons, in events with lower  $\cancel{E}_T$ , an angular separation is required between the  $\cancel{E}_T$  and the leptons. If same-flavour lepton pairs fall within an invariant mass window corresponding to the  $Z$ , an additional  $\cancel{E}_T$  significance cut is made. Events having a jet with  $E_T > 15 \text{ GeV}$  are rejected. Although this increases the purity of the sample it does introduce a systematic uncertainty in the acceptance as measured using simulation, as jet multiplicity is not particularly well-modeled in generators. In  $184 \text{ pb}^{-1}$ , 17 events are observed, with a signal to background ratio of  $\sim 2.3$ , compared with a Standard Model prediction of  $16.1 \pm 1.6$  events. The preliminary resulting cross-section is  $\sigma \cdot Br(p\bar{p} \rightarrow WW) = (14.2_{-4.9}^{+5.6}_{\text{stat}} \pm 1.6_{\text{sys}} \pm 0.9_{\text{lum}}) \text{ pb}$ , to be compared with a NLO prediction<sup>3</sup> of  $(12.5 \pm 0.8) \text{ pb}$ .

The second analysis selects a tight electron or muon having  $E_T > 20 \text{ GeV}$  as previously described, but makes the looser requirement of only an isolated track for the second leg, increasing the acceptance compared with the ‘tight lepton’ analysis and giving some sensitivity to taus, but introducing a large uncertainty associated with the fake-rate. Events with more than one jet having  $E_T > 20 \text{ GeV}$  are rejected, but single-jet events are allowed. Lepton candidates are required to have opposite charge, a requirement is made on the angle between the  $\cancel{E}_T$  and the

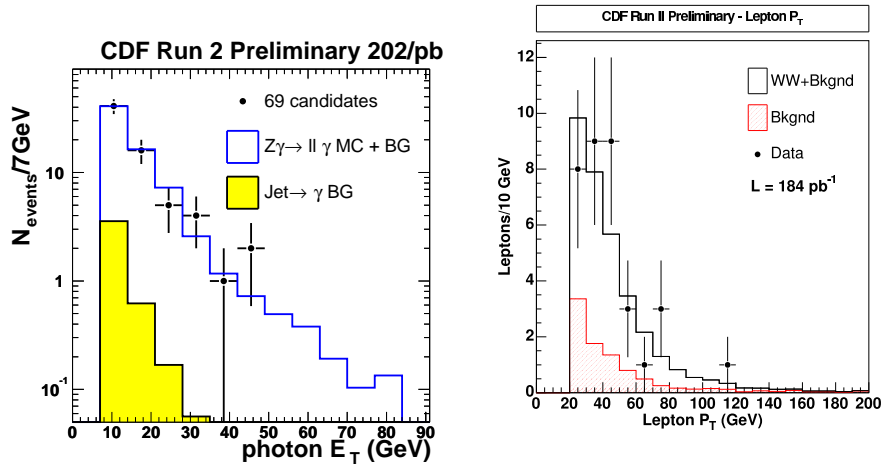


Figure 2: (left)  $E_T^\gamma$  of CDF's  $Z\gamma$  candidate events; (right) Lepton  $p_T$  spectra for CDF's WW candidate events (tight lepton analysis).

lepton candidates, and in the Z mass window an extra requirement is placed on the  $E_T$  significance. 39 events are selected in  $200\text{pb}^{-1}$  with a signal to background ration of  $\sim 1.1$ , compared with a Standard Model prediction of  $31.5 \pm 1.0$  events. The preliminary resulting cross-section is  $\sigma \cdot Br(p\bar{p} \rightarrow WW) = (19.4 \pm 5.1_{\text{stat}} \pm 3.5_{\text{sys}} \pm 1.2_{\text{lum}})$  pb, to be compared with a NLO prediction of  $(12.5 \pm 0.8)$  pb. The lepton  $p_T$  spectrum for the 'tight lepton' analysis is shown in Fig. 2.

## 5 Anomalous Coupling Limits.

Work is in progress on the extraction of anomalous coupling limits from the measured diboson cross-sections. Although LEP data were used to set good limits on anomalous couplings, the Tevatron can produce some events at much higher invariant mass than at LEP and also can probe the WWZ vertex alone, and thus has rather different sensitivity.

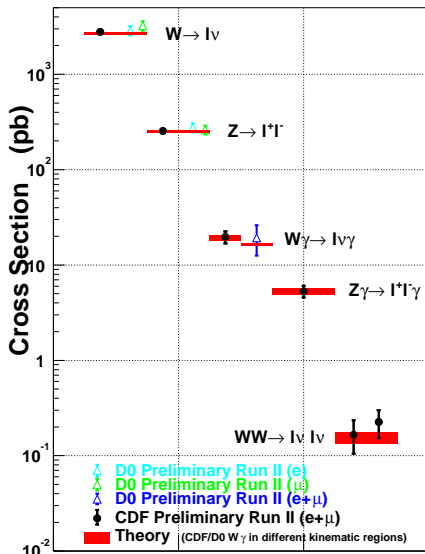


Figure 3: Winter 2004 electroweak cross-section measurements from CDF and D0.

## 6 Conclusions

The electroweak cross-section measurements from the Tevatron for Winter 2004 are summarised in Fig. 3. Diboson cross-section measurements are getting to the point where they are precision measurements; measurements have been made of the  $W\gamma$ ,  $Z\gamma$  and WW cross-sections in the electron and muon channels, and all results are consistent with Standard Model expectations. Anomalous coupling limits will follow.

## References

1. Gavin Hesketh, these proceedings.
2. U. Baur *et al.*, *Phys. Rev. D* **48** 5140 (1993).
3. J. M. Campbell, R. K. Ellis, *Phys. Rev. D* **60** 113006 (1999).